

A measurement of two-photon effects in unpolarized elastic electron-proton scattering

J. Arrington (Spokesperson), D. F. Geesaman, K. Hafidi, R. J. Holt, H. E. Jackson, D. H. Potterveld, P. E. Reimer, E. C. Schulte, X. Zheng
Argonne National Laboratory, Argonne, IL

M. E. Christy, C. E. Keppel
Hampton University, Hampton, VA

G. Niculescu, I. Niculescu
James Madison University, Harrisonburg, VA

R. Ent, D. Gaskell, A. F. Lung, D. J. Mack, D. G. Meekins, G. Smith
Jefferson Laboratory, Newport News, VA

R. E. Segel, I. Qattan
Northwestern University, Evanston, IL

R. Asaturyan, H. Mkrtchyan, V. Tadevosyan, T. Navasardyan
Yerevan Physics Institute, Armenia

(Dated: May 21, 2004)

Abstract

We propose a high precision measurement of elastic electron-proton scattering over a wide range in ε and Q^2 . Deviations of the reduced cross section from linearity are expected if there are sizable two-photon corrections, as has been proposed as an explanation of the discrepancy between Rosenbluth and polarization transfer measurements of the proton form factors. This measurement will provide a significant increase in the sensitivity to deviations from linearity, allowing us to test for the presence of two-photon effects, and provide tight constraints on models of the ε -dependence of the two-photon exchange corrections. Based on recent calculations of the two-photon exchange terms, we expect that the measurement will be able to observe nonlinearities of more than four standard deviations at both $Q^2 = 1.12$ and 2.56 GeV². If no nonlinearity is observed, we will set limits tight enough that the nonlinearities have almost no impact on the extraction of the form factors from a combined analysis of Rosenbluth and polarization transfer data.

In addition, the proposed measurements will allow significantly improved Rosenbluth extractions of $\mu_p G_E/G_M$ for $0.9 < Q^2 < 6.6$ GeV². This data will allow a precise determination of the difference between Rosenbluth and polarization transfer measurements of the form factors. If the discrepancy between the two techniques is related to two-photon exchange effects then this data can be used to extract the two-photon exchange amplitudes. We can then use these amplitudes to apply corrections to the measured form factors and extract the true form factors with minimal uncertainty coming from the two-photon corrections.

I. INTRODUCTION

Recent polarization transfer measurements of the proton electromagnetic form factors at Jefferson Lab [1, 2] have led to significant new activity in modeling of the proton structure. Several new pictures have emerged, highlighting the role of relativity and angular momentum, and the ‘shape’ of the proton (For a review of the theoretical work, as well as details of the experiment, see Ref. [3]). However, these new measurements are in significant disagreement with previous extractions of the form factors that utilized the Rosenbluth separation technique (Fig. 1). Until we adequately understand the discrepancy between the experiments, we cannot be completely confident in our knowledge of the form factors, or the conclusions drawn from them about the role of relativity and quark angular momentum in the proton.

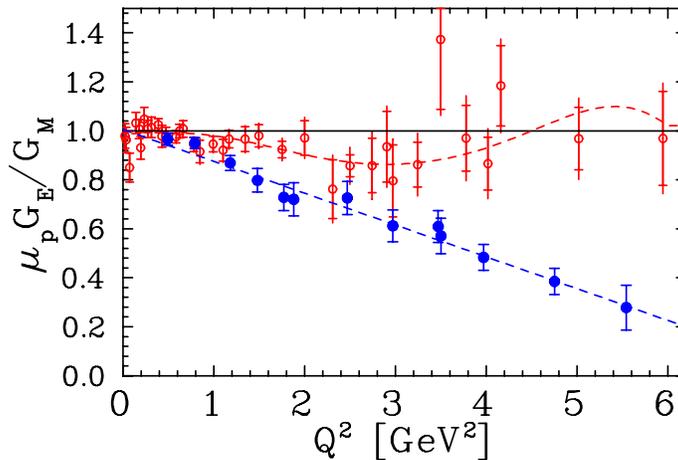


FIG. 1: $\mu_p G_E / G_M$ as deduced from a global Rosenbluth analysis [4] (open circles) compared to the polarization transfer extractions from [1, 2, 5] (filled circles). The outer error bars include an estimate of the uncertainty associated with the determination of the normalization factors for different measurements.

In addition to the implications of the polarization transfer data on the structure of the proton, precise knowledge of the form factors is also important for many other experiments. The elastic cross section is often used as a check of experimental normalizations, and the difference between the Rosenbluth form factors and those extracted from polarization transfer could conceivably have significant impact, up to $\sim 5\%$ or more, on the normalization of several experiments. There are also many cases where precise knowledge of the elastic form factors is assumed in analyzing or interpreting data from other measurements, such as quasielastic scattering. Errors in the elastic form factors can have a significant impact on such experiments, especially if the ε -dependence is important [4, 6]. Finally, if the discrepancy is due to a problem in either the Rosenbluth separation or polarization transfer formalism, then this could have implications for other measurements that use the same techniques.

Because of the difficulty in performing Rosenbluth extractions at large Q^2 and the apparent inconsistencies between different Rosenbluth experiments, it was argued that the discrepancy was due to experimental problems in the Rosenbluth extraction. However, the systematic uncertainties of both the Rosenbluth [7] and polarization transfer [3] measurements have been studied in detail, and no explanation for the discrepancy in terms of

experimental problems has been found. In addition, while the traditional Rosenbluth separation measurements are very sensitive to systematic uncertainties at large Q^2 , a recent ‘‘Super-Rosenbluth’’ measurement [8] was performed in Hall A, which is significantly less sensitive to the dominant sources of uncertainty in the traditional Rosenbluth measurements. Preliminary results from this experiment indicate good agreement with previous Rosenbluth measurements. This demonstrates that the discrepancy is not caused by experimental errors or analysis issues that were suggested when the polarization transfer results initially came out, and would appear to point to a more fundamental problem with one of the techniques.

Analyses of the discrepancy that assume the difference is due primarily to missing corrections in the cross section measurements [4, 7, 9] indicate that the discrepancy could be explained by an error in the ε -dependence of the cross section of approximately 5–8% for $1 < Q^2 < 6 \text{ GeV}^2$. The correction would have to lower the measured cross section at high ε relative to low ε , and be close enough to linear that it does not spoil the linearity from the Rosenbluth formula (see Fig. 2). Coulomb corrections, when implemented in a simple effective momentum approximation [10] or using a more detailed approach [11], do modify the ε -dependence of the cross section, but yield a very small effect compared to the size needed to explain the discrepancy. For the most part, investigations have focussed on the effect of two-photon exchange corrections [9, 12–15] beyond those included in the traditional calculations of radiative corrections (e.g. Ref. [16]).

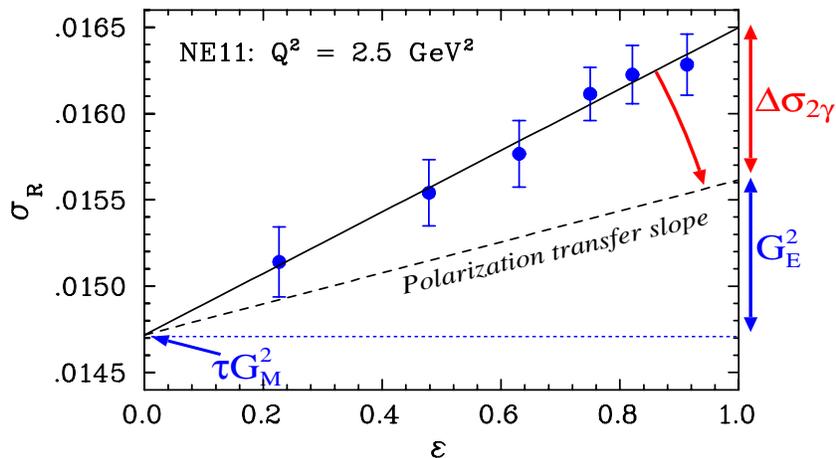


FIG. 2: The ε -dependence of the reduced cross section as predicted from the polarization transfer results for G_E/G_M (dashed line), and as measured in SLAC NE11.

One way to look for two-photon effects in the unpolarized cross section is to look for deviations from linearity in the ε -dependence of the reduced cross section. We propose a measurement that will have significantly greater sensitivity to two-photon effects in the linearity of the ε -dependence: a factor of six increase in the sensitivity over published measurements, and a factor of three to four over than projected results from E01-001 [8]. Based on estimates of the nonlinearities, discussed in Section III, the sensitivity should be enough to see these effects at the four sigma level at both $Q^2 = 1.12$ and 2.56 GeV^2 .

In addition to mapping out the ε -dependence of the two-photon contributions, we can also extract the Q^2 -dependence by combining the high-precision Rosenbluth measurements with existing high-precision polarization transfer data. Such an analysis has been performed using existing data [9, 17], but the current data do not allow for a precise measurement of the

two-photon exchange corrections. The main limitations in such an analysis are uncertainty in the ε -dependence of the two-photon corrections, and the large uncertainty in Rosenbluth separation measurements of G_E/G_M at moderate to large Q^2 values. This proposal will address these issues by directly testing the assumption of linearity in the correction, and by providing improved Rosenbluth measurements of G_E/G_M in the region where the current data are not precise enough to extract two-photon contributions. Any observed nonlinearity can be incorporated into these extractions, and if we do not observe nonlinearities, then we know that the assumption of linearity in the extraction will not cause significant uncertainties in the extracted form factors.

There are two main aspects to the proposed measurements. First, we will perform a high precision test of the linearity of the Rosenbluth separation at two Q^2 values, sensitive enough to detect the nonlinearities estimated from current calculations at the four sigma level. This data will provide strong constraints for models of the two-photon effects on the unpolarized cross section. Mapping out the ε -dependence will also minimize the assumptions that go into extracting the two-photon amplitudes from the discrepancy. In addition, the experiment will provide high-precision Rosenbluth extractions of G_E/G_M , which will significantly improve the precision with which we can extract the two-photon amplitudes based on the comparison of Rosenbluth and polarization transfer results, which will in turn allow us to correct the measurements of the proton form factors with significantly smaller uncertainties associated with the two-photon corrections. The high precision measurements of G_E/G_M will not only improve the extraction of the two-photon amplitudes from the discrepancy, they will allow us to extract the size of the two-photon corrections for lower Q^2 values, where the current uncertainties on the Rosenbluth separation measurements make it difficult to determine if there is any discrepancy at all. This will greatly aid comparisons with existing (or future) positron measurements which are also sensitive to the two-photon contributions, but which are extremely difficult to perform at large Q^2 and small ε , where the two-photon effects appear to be large. Mapping out the two-photon effects over a range in ε and Q^2 will also allow us to test two-photon calculations, which can then be applied to other reactions.

The main goal of this proposal is to extract the true proton form factors. We will do this by measuring G_E/G_M and the ε -dependence of the reduced cross sections well enough to constrain the ε and Q^2 dependence of the two-photon amplitudes. With the proposed measurements, we should be able to extract G_E and G_M with uncertainties related to the two-photon effects that are comparable to or smaller than the experimental uncertainties. Such an extraction using existing data is discussed in the appendix (submitted separately). Section V C summarizes the limitations of such an analysis, given the current data, and shows how the proposed measurement can both test the assumptions and significantly improve the precision of such an extraction of the two-photon corrections.

II. SIGNATURES OF TWO-PHOTON EXCHANGE CONTRIBUTIONS

Two-photon exchange contributions to elastic electron-proton scattering can be observed in several different ways. The real part of the two photon amplitudes modifies the polarized and unpolarized cross sections, and the polarization transfer components used to extract G_E/G_M . The imaginary part of the amplitudes leads to non-zero values for the Born-forbidden A_y (or P_N). These observables provide a clean measurements of two-photon effects, but are not directly connected to the real part of the two-photon amplitudes which may be responsible for the discrepancy in the proton form factor extractions.

There are two ways to look for the effects of two-photon corrections in the *unpolarized* elastic e-p cross section. First, one can compare positron-proton and electron-proton scattering. Interference terms between one-photon and two-photon exchange will have the opposite sign for positron-electron scattering, and will lead to a difference in the electron and positron cross sections. Such measurements require a precise comparison of positron and electron scattering, and have been limited by the luminosity of the secondary positron beams used for such measurements. Additional comparisons of positron to electron scattering over a range in Q^2 and ε would provide the most direct extraction of these two-photon corrections. Unfortunately, there is currently no way to make adequate positron measurements over the Q^2 range where the existing measurements show a clear discrepancy.

Alternatively, one can test the linearity of the reduced cross section as a function of ε . In the Born approximation, the reduced cross section should be a linear function of ε , and deviations from linearity would indicate a correction to the Born approximation that is not taken into account in the radiative corrections. This is not as direct a measurement as the comparison of positron to electron scattering, but an observation of a nonlinearity would provide a clear signature of deviations from the Born approximation, and would provide information on the nonlinear component of the two-photon contributions.

A. Experimental limits on nonlinearities

Several experiments have looked for two-photon exchange terms in the linearity of the Rosenbluth plot. Previous measurements have not shown any significant deviations from linearity, but have been limited by the size of the uncertainties and the ε range covered by most experiments.

To compare the proposed measurement to existing data, we need a figure of merit for the sensitivity to nonlinearities. We perform a quadratic fit to the ε -dependence of the data, and use the uncertainty of the quadratic term as an indication of the sensitivity of a given dataset to nonlinearities. For a fit of the form

$$\sigma_R = P_0[1 + P_1\varepsilon + P_2\varepsilon^2] \quad (1)$$

P_2 determines the relative size of any nonlinear contributions, and δP_2 can be used to set limits on such terms. Previous measurements have found P_2 to be consistent with zero, with $\delta P_2 > 0.100$. This yields limits on nonlinearities of $\sim 2.5\%$, if the deviations from linearity are symmetric about $\varepsilon = 0.5$, and if the data covers a symmetric range about $\varepsilon = 0.5$. The data provide weaker limits if the nonlinearities occur only at large (or small) ε values or if the data has an asymmetric ε range (as seen in Fig. 3). In addition, for a more complicated ε -dependence, the *size* of the extracted curvature parameter P_2 will depend on the ε range covered. The proposed measurement will dramatically reduce the uncertainties on P_2 , yielding an uncertainty of $\delta P_2 < 0.020$.

The best extraction of the ε -dependence at large Q^2 is from SLAC NE11 [18] (Fig. 3). The data at $Q^2 = 2.5 \text{ GeV}^2$ yield $P_2 = 0 \pm 0.105$. The dashed lines show the best fits with $P_2 = \pm 0.105$, and the deviations from the linear fit are $\pm 3\%$ at $\varepsilon = 0$, $\pm 1.3\%$ at $\varepsilon = 1$. The measurement by Walker, *et al.*, [19] did not have data below $\varepsilon = 0.6$, while the recent JLab E94-110 measurement [20], which was designed to perform L-T separation over the resonance region, does not have enough ε points at a given Q^2 value to set strong limits. By combining their data over a range in Q^2 (2.5–3.5 GeV^2) there is enough ε range, and the

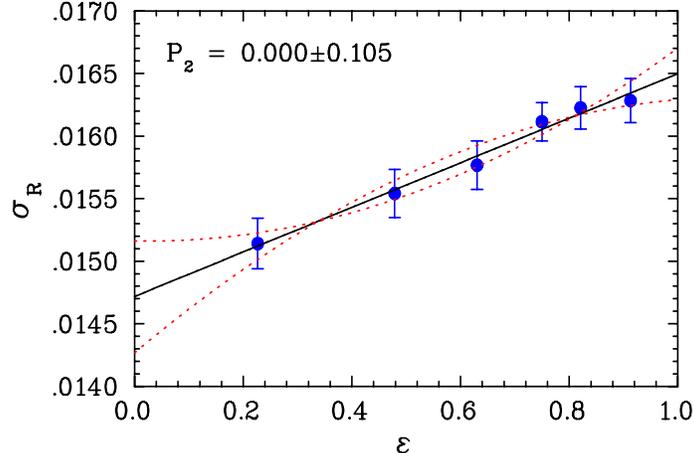


FIG. 3: The ε -dependence of the reduced cross section from NE11 (using only the data from the 8 GeV spectrometer). The solid line is the linear fit, while the dashed lines are quadratic fits with $P_2 = \pm 0.105$ (one-sigma variations from the central value).

uncertainty on the quadratic terms is similar to the NE11 limit, though with a somewhat larger average Q^2 . Similar limits can be placed on nonlinearities at lower Q^2 from Berger, *et al.* [21]. They measured the linearity of the Rosenbluth plot at several Q^2 values below 1 GeV², and found P_2 to be consistent with zero, with uncertainties that varied between 0.120 and 0.250 for $Q^2 \approx 0.4, 0.6, 0.8,$ and 1.0 GeV².

E01-001 [8] will provide an improved limit on nonlinearities. At $Q^2 = 2.64$ GeV², there are five points for $0.12 < \varepsilon < 0.87$. The projected uncertainties in the E01-001 proposal are approximately 0.8%, which lead to an uncertainty in P_2 of 0.064, almost a factor of two better than previous measurements. Although this experiment has significantly smaller uncertainties than previous measurements, the ε range of the data and the limited number of ε points taken significantly limit the sensitivity of the E01-001 measurement. The E01-001 data typically have sensitivity to nonlinearities only in one or two points. For a precise measurement of the nonlinearities, it is important to minimize the uncertainties and have many points covering the maximum possible ε range so that one is sensitive to nonlinearities at both large and small ε values, and so that there will be several points in any linear region to act as a precise ‘baseline’ for nonlinearities.

One can attempt to combine different experiments in a global analysis to increase the sensitivity to small nonlinearities. However, while uncertainties in the overall normalization drop out when examining a single dataset, this is not true in a combined analysis of multiple datasets. Typically, global analyses use the consistency of the datasets in order to extract the relative normalizations of different experiments. However, this has always involved assuming a *linear ε -dependence* to compare datasets at different kinematics. Such an assumption will systematically tend to mask any real nonlinearity, making it difficult to set meaningful limits from such a global analysis. The data can be combined without adjusting the normalization factors for each experiment, and then the uncertainty arising due to the normalization factors can be estimated by varying the normalization of each data set and using the change in the fit to estimate the uncertainty. However, this leads to systematic uncertainties which are larger than the total uncertainties from the analysis of a single, high-precision, data set.

B. Positron to electron comparisons

The main effect of two-photon exchange on the cross section comes from the interference between the one-photon and two-photon exchange amplitudes, $M_{1\gamma}$ and $M_{2\gamma}$:

$$\sigma(e^\pm p) = |M_{1\gamma} \pm M_{2\gamma}|^2 \approx M_{1\gamma}^2 (1 \pm 2\text{Re}(M_{2\gamma}/M_{1\gamma})). \quad (2)$$

Because the sign of the correction depends on the lepton charge, the ratio of positron to electron scattering, $R \equiv \sigma(e^+p)/\sigma(e^-p) \approx 1 + 4\text{Re}(M_{2\gamma}/M_{1\gamma})$, is very sensitive to two-photon exchange effects. In the simplest approximation, one expects the two-photon amplitude to be suppressed by an additional factor of α , leading to a decrease of $2\alpha \approx 1.5\%$ in the electron cross section, and an increase of $4\alpha \approx 3\%$ in the ratio R .

If we assume that two-photon corrections are responsible for the discrepancy between polarization transfer and Rosenbluth measurements, we can make specific predictions about how these corrections would affect the positron measurements. To explain the discrepancy, the effect must increase the slope of the Rosenbluth plot, and so must either increase the electron cross section at large ε or decrease the cross section at low ε . Based on the size and Q^2 -dependence of the discrepancy, the ε -dependence of the effect must be 5–8%, depending only weakly on Q^2 , for $Q^2 \gtrsim 2 \text{ GeV}^2$. It must also be reasonably close to linear in ε , or else it would introduce nonlinearities in the Rosenbluth plot. This implies that the positron to electron ratio should have a 10–15% ε -dependence, roughly linear in ε , which increases the ratio at small ε relative to large ε .

Existing comparisons of positron- and electron-proton scattering yield an average ratio of $\langle R \rangle = 1.003 \pm 0.005$, with $\chi_\nu^2 = 0.87$. These data have been interpreted as showing that the two-photon corrections must be even smaller than the naive estimate, and thus well below the level necessary to explain the discrepancy. The same is true of μ^+p and μ^-p comparisons, which are also consistent with $R = 1$ [22].

Unfortunately, the low intensity of the secondary positron (and muon) beams make precise measurements difficult in regions where the cross section is small. Because of this, all of the positron data are for low Q^2 ($Q^2 < 1.3 \text{ GeV}^2$) or small scattering angles ($\varepsilon > 0.7$). So while the existing data do place fairly tight limits on the size of two-photon corrections in some regions, two-photon effects are not well constrained at large Q^2 or low ε . In Fig. 4, the data for $Q^2 < 2 \text{ GeV}^2$ are plotted as a function of ε , and a significant ε -dependence can be seen [23]. A linear fit, neglecting any Q^2 -dependence, yields an ε -dependence of $-(5.7 \pm 1.8)\%$, with $\chi^2 = 11$ for 22 degrees of freedom. While this is roughly half of the effect needed to explain the form factor discrepancy at high Q^2 , the average Q^2 value for the low ε data is 0.5 GeV^2 , a factor of 5–10 lower than the Q^2 values where there is a clear discrepancy in the form factor measurements. Given that recent attempts to calculate the two-photon corrections indicate a weak Q^2 -dependence (Sec. III), this reduction in the effect at very low Q^2 is consistent with what one might expect given the observed discrepancy at larger Q^2 .

While we cannot make a direct comparison of the two-photon corrections implied by the positron measurement to those necessary to explain the form factor discrepancy, these data yield important information on these two-photon corrections. The observed ε -dependence in R provides evidence for large two-photon corrections in the elastic cross sections, and supports the idea that they may explain the discrepancy between polarization transfer and Rosenbluth separation measurements. If we combine this information with the observed discrepancy between cross section and polarization data, we can estimate the size of the

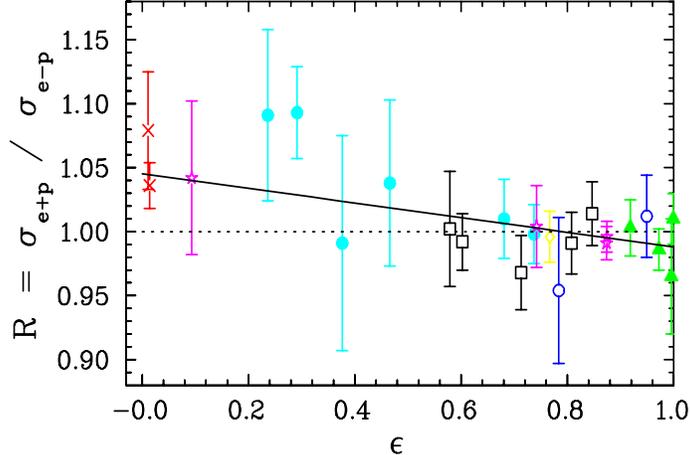


FIG. 4: The ratio $R = \sigma_{e^+}/\sigma_{e^-}$ as a function of ε for the measurements below $Q^2 = 2 \text{ GeV}^2$. The solid line is a fit assuming a linear ε -dependence and no Q^2 -dependence to the ratio, and yields a slope of $-(5.7 \pm 1.8)\%$.

two-photon amplitudes, and estimate the corrections (and uncertainties) that need to be applied to extract the form factors [17].

III. ESTIMATES OF THE TWO-PHOTON EXCHANGE CORRECTIONS

In the 1950s and 1960s, several papers estimated the size of two-photon contributions to the unpolarized cross sections, including only the unexcited intermediate proton state [24], or including excitations of the intermediate state [25–28]. In general, the predicted two-photon effects were consistent with the a small differences between positron and electron scattering, and were too small to introduce observable nonlinearities. In the last year, a significant amount of work has gone into improving such calculations [12, 14, 15], or attempting to make model-independent statements about the form of such corrections [9, 13]. All of the new calculations that provide predictions for the ε -dependence of the two-photon corrections yield noticeable nonlinearities.

Calculations by Blunden, Melnitchouk, and Tjon [12] yield an ε -dependence of $\approx 2\%$, with small nonlinearities at low ε values. With the inclusion of improved form factors, these corrections increase to $\approx 3\%$ [29]. This calculation yields almost no correction at $\varepsilon \approx 1$, and a decrease at low ε values, consistent with what is observed in the positron to electron ratios. There is a small Q^2 -dependence to the slope at large Q^2 , parameterized by $\ln(Q^2/0.65)$ for $Q^2 > 1\text{--}2 \text{ GeV}^2$. However, these calculations include only the elastic portion of the two-photon correction, i.e. the box and crossed-box diagrams with the proton in the intermediate state, and neglect intermediate states which have been shown to be important in other processes in certain kinematic regimes [30, 31].

Calculations at the quark-parton level in the double logarithm approximation by Afanasev [15] yield a different form for the ε -dependence. Again, the two-photon correction is nearly linear over most of the ε range, and is small at large ε values, and so is not ruled out by positron measurements. However, it yields a very different nonlinearity from the calculation of Ref. [12].

A recent preprint [14] calculates the TPE effect at the quark-parton level, using a gen-

eralized parton distribution to describe the emission and re-absorption of the partons by the nucleon. While this approach is not expected to be valid at low Q^2 or ε values, the calculations for higher Q^2 again show a significant ε -dependence to the correction, with only a weak Q^2 -dependence.

We use these calculations to estimate the size of possible nonlinearities in the ε -dependence. While they yield different forms for the nonlinearities, they all agree that the correction is small for large ε values, decreases the measured cross section at small ε values, and depends only weakly on Q^2 (at least for large Q^2 values). The calculation of Ref. [15] provides only the form of the ε - and Q^2 -dependence, but not the overall magnitude. The other calculations do predict the magnitude of the corrections, but both yield approximately half of the effect necessary to explain the discrepancy between Rosenbluth and polarization transfer. To use these as estimates of the nonlinearity, we have scaled all of the calculations such that the overall correction to the Rosenbluth measurements is sufficient to explain the observed discrepancy. Specifically, the calculations are scaled such that the linear portion of the correction over the ε range of previous measurements yields correction of approximately 6% to the slope.

Figure 5 shows the ε -dependence of these calculations. Also shown are the ε values and projected uncertainties for the E01-001 measurement at $Q^2 = 2.64 \text{ GeV}^2$, arbitrarily placed on the Afanasev curve. Note that the calculation of Ref. [14], the curve for $Q^2 = 2.5$ only extends down to $\varepsilon = 0.46$, which makes it difficult to determine the ε -dependence. To improve the ε range, we take their calculation at $Q^2 = 5 \text{ GeV}^2$, which extends down to $\varepsilon = 0.26$, and extend the curve linearly to $\varepsilon = 0$.

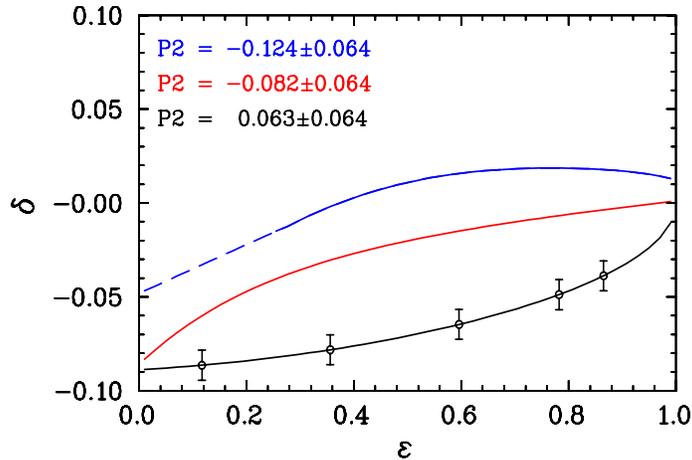


FIG. 5: The two-photon exchange contribution ($\delta = [\sigma_{Born+2\gamma} - \sigma_{Born}]/\sigma_{Born}$) to the elastic electron-proton cross section from the calculations of Blunden, *et al.*, [12, 29] (red (middle) curve), Afanasev [15] (black (bottom) curve), and Chen, *et al.*, [14] (blue (top) curve) after scaling the calculations to yield a ε -dependence of $\sim 6\%$ over the ε range of existing data. The circles indicate the kinematics and proposed uncertainties (at $Q^2 = 2.64 \text{ GeV}^2$) for E01-001.

From Fig. 5, it is clear that the size of the extracted nonlinear term will depend on the ε range covered, as the various calculations show nonlinearities in limited (but different) regions of ε . By placing the points from E01-001 on one of the curves, we can make a quadratic fit to the pseudo-data and determine the curvature that would be seen in the experiment for each of the calculations. The extracted values of P_2 are shown in the figure

for each of the three curves. The projected results from E01-001 are only sensitive to these nonlinearities at the 1–2 sigma level. Previous experiments, which yielded uncertainties on P_2 of 0.100 or larger are only sensitive to the predicted curvatures at the one-sigma level. The proposed experiment will measure P_2 with a very small uncertainty, $\delta P_2 \leq 0.020$, at two different Q^2 values. This corresponds to a four to six sigma measurement of the curvature, depending on the model one uses. In addition, because the models vary in the sign of the curvature, the range of P_2 values is 0.187, almost 10 times the precision of the proposed measurement.

IV. EXPERIMENT

The proposed measurement is a conventional Rosenbluth separation, but instead of detecting the scattered electron, we will detect the struck proton. Detecting the proton reduces several ε -dependent systematic uncertainties. The major sources of uncertainty in the most precise SLAC measurements [18, 19] were statistics at low ε , uncertainty in the scattering kinematics, the total charge, corrections that depended on rate or kinematics, and the target density. Because we measure the protons, we are less sensitive to knowledge of the scattering kinematics, and have a constant proton momentum. In addition, the cross section is nearly constant when detecting the proton, so that any rate-dependent corrections will yield minimal ε -dependence. It also means that we can use a constant beam current, which will reduce the relative uncertainty in the luminosity at different ε values.

The first goal of the proposed experiment is to make an improved measurement of any nonlinearity in the ε -dependence. Current measurements of the curvature yield $\delta P_2 > 0.100$ for both small and moderate Q^2 values. Experiment E01-001 will reduce this to 0.064 for $Q^2 = 2.64 \text{ GeV}^2$. The projected uncertainties for this proposal yield $\delta P_2 = 0.020$ (0.018) for $Q^2 = 2.56 \text{ GeV}^2$ (1.12 GeV^2). By increasing the ε range of the data, the number of ε points, and reducing the ε -dependent systematics, we will have a sensitivity of four standard deviations to each of the forms shown in Fig 5. In addition, while the curvature of the quadratic fit is a useful general measure of the nonlinearities, we can provide better discrimination against specific models.

The second goal is to provide additional, high precision, L-T separations for $1 \lesssim Q^2 \lesssim 6 \text{ GeV}^2$. This will allow a more precise extraction of the two-photon effects from the difference between Rosenbluth and polarization transfer measurements. Such a determination, necessary for a precise extraction of the proton form factors, must start with several assumptions [17]. The proposed measurement will provide the ε -dependence of the correction to the cross section data, either by measuring nonlinearities, or by setting tight limits on deviations from linearity. In addition, it will allow a determination of the Q^2 -dependence of the two-photon effects by providing improved Rosenbluth measurements of $\mu_p G_E/G_M$. The proposed measurements will increase the precision on G_E/G_M by roughly a factor of two over the entire Q^2 range compared to a global Rosenbluth of the world's body of high- Q^2 cross section data. This will allow a precise comparison with polarization transfer measurements and, combined with limits from existing positron-proton data, will allow us to extract the two-photon amplitudes well enough to correct the extracted values of G_E and G_M for two-photon contributions.

A. Experimental equipment

The experiment is proposed for Hall C using the HMS spectrometer and the standard cryogenic targets. The 4 cm liquid hydrogen target will be viewed at a maximum angle of 60 degrees, so target length effects on the acceptance (after our solid angle and momentum acceptance cuts) will be negligible. Time of flight and an Aerogel detector will be used for p/π separation. Solid angles will be restricted to about 3.2 msr by software cuts. Coincidence data will be taken at some kinematics to check our modeling of the background, the spectrometer resolution, and the radiative tail for the elastic peak.

B. Advantages of proton detection

For this measurement, proton detection has several advantages over electron detection. Table I compares the electron kinematics to the proton kinematics for the two Q^2 values where we propose to make precise linearity tests, while Figure 6 shows the ε -dependence of the cross section, sensitivity to angle, and spectrometer momentum for electron detection and proton detection. To detect the electron, we would have to go to extremely large scattering angles to obtain the small ε data. This means that we would have to detect electrons from roughly 350 MeV to more than 5 GeV, and so any momentum-dependence in the optics, detector efficiency, or particle identification would introduce an additional ε -dependence. For protons, the momentum at a fixed Q^2 is constant. In addition, at large electron angles the cross section is extremely small. The cross section for the proton is much less dependent on ε , leading to three significant advantages: (1) the minimum cross section is 10–20 times higher for the proton than for the electron, (2) the maximum cross section is much lower, meaning that any rate-dependent efficiency correction will be smaller and introduce less ε -dependence, and (3) the small variation of cross sections with ε means that we can run at fixed beam current, reducing the ε dependence of any corrections due to target heating or BCM nonlinearities.

	$Q^2 = 1.12 \text{ GeV}^2$ settings		$Q^2 = 2.56 \text{ GeV}^2$ settings	
	Proton	Electron	Proton	Electron
ε	0.05–0.98	0.05–0.98	0.08–0.93	0.08–0.93
p [GeV/c]	1.21	0.34–5.47	2.10	0.46–4.70
σ_{min}	3.9 nb/sr	0.30 nb/sr	0.30 nb/sr	0.014 nb/sr
$\sigma_{max}/\sigma_{min}$	2.5	370	1.7	140
$\Delta\sigma/\Delta\theta$	0.4–1.6 %/mr	-(0.1–4.2)%/mr	0.7–1.7 %/mr	-(0.1–2.8)%/mr

TABLE I: Comparison of electron and proton kinematics for the $Q^2=1.12 \text{ GeV}^2$ and $Q^2 = 2.56 \text{ GeV}^2$ measurements.

The uncertainty in the scattering angle was one of the largest sources of uncertainty in previous measurements where the electron was detected. For our kinematics, the electron cross section can vary by up to 4.2% for a 1 mr error in the scattering angle. For the proton, the size and ε -dependence of this correction are typically a factor of two or more smaller, and the ε -dependence is roughly linear (Fig. 6). So not only is the correction due to a constant angle offset reduced by a factor of two or more, the deviations from linearity are

smaller still. Finally, because the scattered electron is not detected the radiative corrections are smaller and much less ε -dependent.

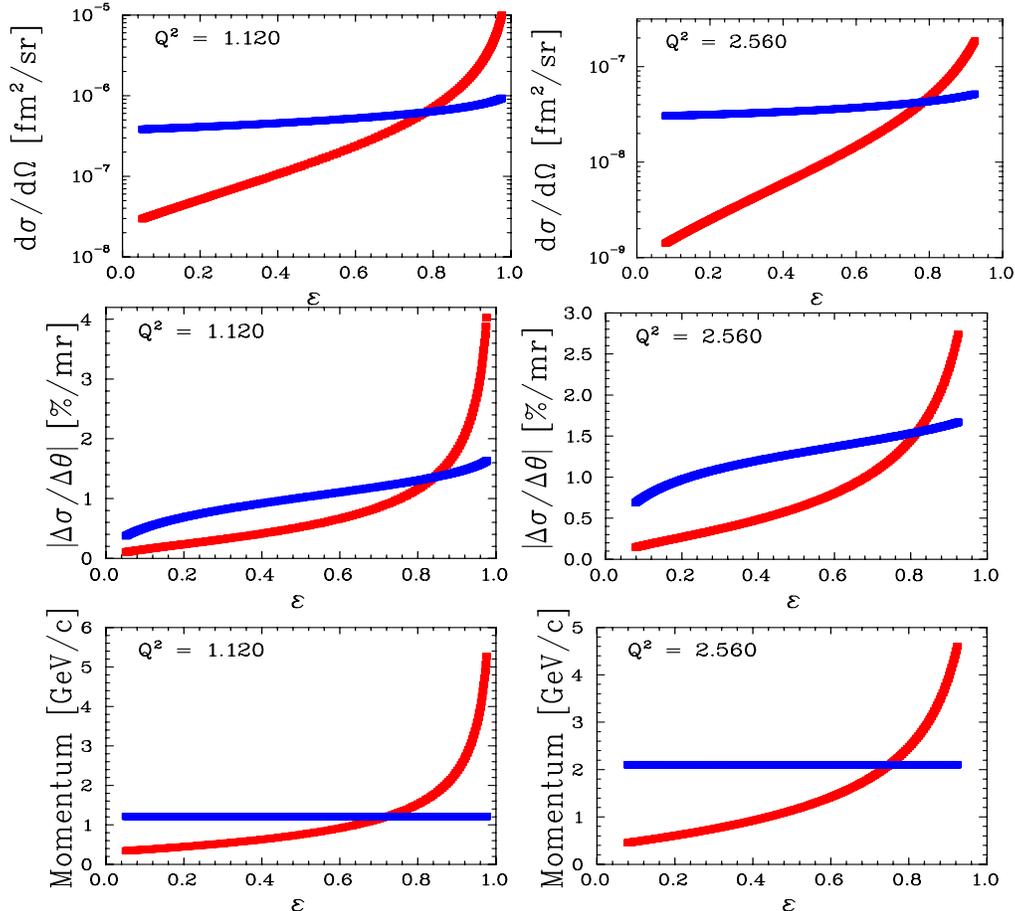


FIG. 6: Cross section (top), sensitivity to angle (middle), and detected particle momentum (bottom) for detection of electrons (red) and protons (blue) at the two Q^2 values where we will make a high precision linearity measurement.

There will be corrections to the absolute cross section that are larger when detecting the proton, but these are very nearly independent of ε . Protons will undergo hadronic reactions and be lost in the target or detector materials. This leads to a loss of $\sim 5\%$ of the protons, which depends almost entirely on the proton momentum. There is a very small ε -dependence because the amount of target material the proton interacts with changes as the proton angle changes. This variation is extremely small ($< 0.1\%$ for E01-001), and is taken into account in the analysis of the experiment.

Protons are not always stopped by the HMS collimator, so one cannot rely on the collimator to define the solid angle for the measurement. We will define the solid angle using cuts on the reconstructed scattering angles, in a region where the HMS has 100% acceptance. While any error in the angular reconstruction will lead to an uncertainty in the *absolute* solid angle, identical cuts will be used at forwards and backwards angle, and the uncertainty in the solid angle will cancel. The software cuts may also yield an additional offset in the average scattering angle, but it will be the same offset for all settings, and because the effect of a fixed shift in the proton angle is relatively small and very nearly linear, the effect on

the linearity test is extremely small.

C. Backgrounds

The biggest drawback in detecting the protons is the presence of background processes that generate protons close to the elastic peak. Figure 7 shows simulated proton singles spectra as a function of the difference between the measured proton momentum and the momentum calculated from the measured angle, assuming elastic scattering. The data are plotted against δp , the difference between the measured proton momentum, and the proton momentum calculated from the measured angle, assuming elastic kinematics. The contribution of the elastic and background processes is matched to the results obtained from E01-001. The elastic events peak near zero, and have a radiative tail (blue dots). These events sit on top of a significant background of events coming from the target endcaps (yellow points). In addition, there are protons coming from Compton scattering (magenta) and neutral pion photoproduction (green).

The contributions from the target endcaps are a larger fraction of the elastic peak than in the case of electron detection, and include both electroproduction and photoproduction processes. We will take adequate measurements with an aluminum ‘dummy’ target, and use a target that more closely matches the radiation length of the hydrogen target in order to minimize the differences between the endcap and dummy target contributions. For the spectrum at 2.64 GeV^2 , the endcap subtraction varies between $\sim 10\%$ at high ε (for $-25 < \delta p < 25 \text{ MeV}$) to $\sim 15\%$ at low ε (for $-15 < \delta p < 15 \text{ MeV}$). With these cuts on δp , we can eliminate most of the background contributions, while staying away from the edges of the elastic peak. With these cuts, there is an ε -dependence of $\sim 5\%$ in the background subtraction. We should be able to measure the endcap contribution to better than 2% , yielding an uncertainty in the slope of $< 0.1\%$, and contributions to the nonlinearity that are smaller, since the size of the dummy subtraction varies approximately linearly with ε .

Photoproduction of neutral pions is the other significant source of high energy protons. For the low Q^2 data, the threshold for pion production is far enough below the elastic peak that it can be easily cut away. For the higher Q^2 values, we will need to subtract away these contributions. Figure 7 shows the simulated spectrum for $Q^2 = 2.64 \text{ GeV}^2$. For forward angle settings (small ε), this background is large, but can be almost entirely cut away with a reasonable cut on the elastic peak. At larger angles, the resolution is worse and the background cannot be cut away. However, at larger angles, the background becomes very small compared to the elastic contribution, and the background can be modeled well enough to subtract away its small contribution. To verify our modeling of the background and the shape of the elastic peak, we can compare a tight cut (excluding the background but sensitive to how well we reproduce the shape of the elastic peak) to a loose cut (insensitive to the resolution, but with larger background contributions) for all kinematics. In addition, we will have coincidence runs at a few kinematics which will allow us to separate the elastic events from the background processes in order to test our calculations of the line shapes.

There will also be a background of charged pions in the HMS. For some kinematics the pion production threshold is far enough below the elastic peak to cleanly separate the pions. Time of flight will efficiently remove pions for the low Q^2 data, and an Aerogel detector will be used to reject pions where the time of flight is not fully efficient. The pion contamination will be negligible after the particle identification cuts, while the inefficiency of the cuts for protons depends only on the proton momentum (i.e. Q^2) and thus does not introduce any

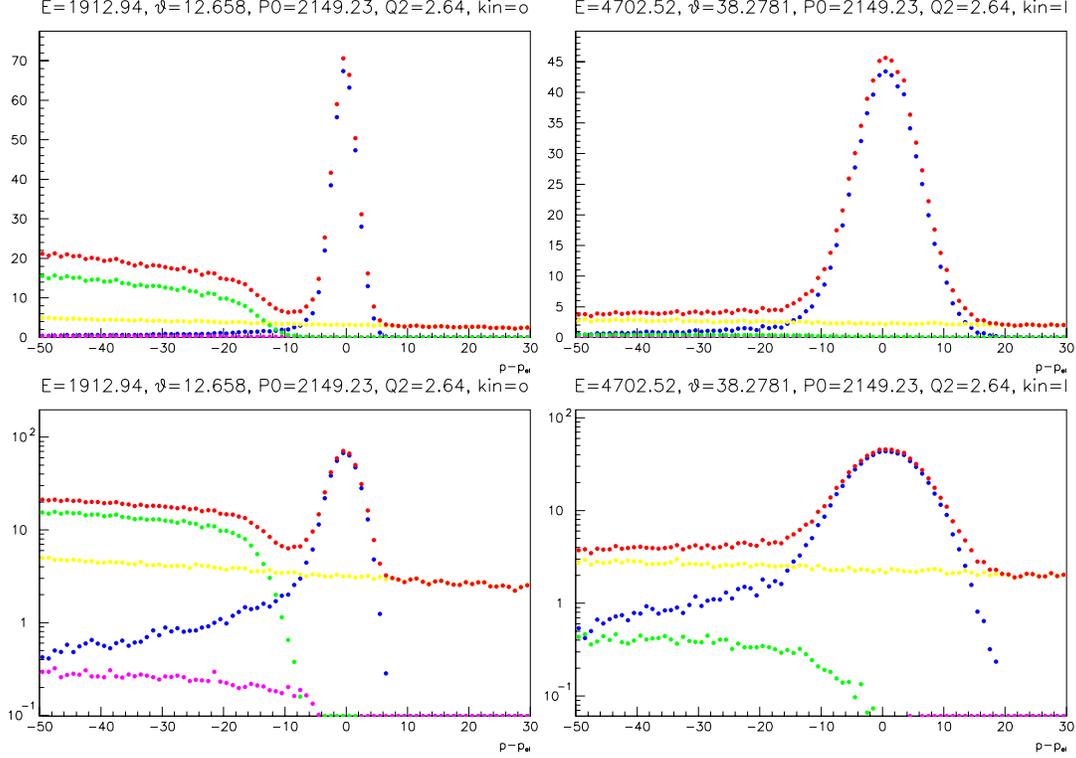


FIG. 7: HMS Proton elastic singles spectra from SIMC on a linear scale (top) and logarithmic scale (bottom). The kinematics are taken from the lowest (left) and highest (right) ε points from E01-001 at $Q^2=2.64$ GeV². The yellow points are the dummy target data (taken from E01-001), while the other points are the dummy data combined with the simulated Compton (magenta), π^0 -p (green), and elastic (blue) simulations. The red points show the sum of the endcap data and all of the simulated processes, all normalized to match the E01-001 results.

uncertainty in the ε -dependence.

D. Systematic uncertainties

Because of the high precision required for this measurement, we have to ensure that we take into account many corrections that are often assumed to be small or negligible. In addition, we must separate out uncertainties which lead to a scale offset for all values at a given Q^2 from those which vary randomly from point-to-point, or those which vary linearly with ε .

Computer dead time corrections are measured in the standard data acquisition system in Hall C. The number of triggers generated and the number of events written to tape are recorded and the cross section is corrected by the fraction of events sampled with a very small associated uncertainty. Electronic dead time is determined by measuring the loss of events for a variety of electronic gate widths (starting at 50 ns, the nominal gate width for the trigger signals) and extrapolating back to zero gate width. A larger problem could be the presence of multiple tracks in the chambers. While the tracking code does a good job of selecting the track that formed the trigger, there can be confusion in the tracking for

overlapping events. The time window over which this could cause problems is 200-300 ns. For this experiment, the rates are low enough that these effects will always be small, and often negligible.

The uncertainty in the luminosity comes mainly from the measurement of the beam current and corrections for fluctuations in the target density. Because the rates are never very large, we can take all of the data at a fixed beam current. Thus, while the absolute uncertainty in the BCM calibration is about 0.5%, the fluctuation over time can be held to 0.2%. The density fluctuations also depend on beam current, so while the uncertainty in the absolute density is a few tenths of a percent, the effect on the L-T separation and the linearity measurement is negligible.

At low Q^2 , the elastic rate over the full (~ 7 msr) solid angle varies from 4 kHz at low beam energy to 10 kHz at high beam energy. However, the inelastic backgrounds are larger at forward angles so the raw event rate, which determines deadtime and tracking inefficiencies, should vary by less than a factor of two. The *maximum* rate will be less than 20 kHz, leading to a small total correction for electronic deadtime ($\sim 0.2\%$) and multiple tracks ($\sim 0.5\%$), with an ε -dependence that is less than half of this size. The uncertainties on these corrections will be less than 0.05%. At larger Q^2 values, the trigger rate is dominated by the inelastic contribution and the maximum rates should be 5 kHz or less, yielding corrections (and uncertainties) a factor of four or more lower.

Significant systematic uncertainties can come from the uncertainty in the scattering kinematics, and so we will require good beam energy stability and beam energy measurements. The sensitivity of the cross sections is typically 4–6% for a one percent change in beam energy, with little ε -dependence. So an overall offset of 0.04% in the beam energy yields a scale uncertainty in the cross section of 0.2%, and an ε -dependent correction of 0.1%, very nearly linear in ε . This linear correction goes into the extraction of G_E/G_M , but not the deviations from linearity. The *linearity* measurement is much more sensitive to uncorrelated beam uncertainties. Assuming a point-to-point beam energy uncertainty of 0.04%, as obtained by E94-110 [20], the cross sections vary by about 0.2%.

The uncertainty in the angle of the scattered proton also breaks down into an overall offset (identical for both forward and backward angles) and an offset that can vary randomly as the spectrometer angle is changed. In addition, because we will define the scattering angle acceptance with software cuts rather than with a collimator, an error in the angle reconstruction will modify the size and central angle for the defined angular acceptance. We will use the same cuts for all kinematics and so the uncertainty in the total solid angle will cancel, but there can still be an overall offset in the central scattering angle of the software restricted window. We expect to achieve an overall offset of 0.3 mr, larger than the 0.2 mr achieved in E94-110 due to the additional uncertainty associated with the software-defined solid angle. We may be able to do slightly better, since we can use the elastic scattering kinematics at each setting as a check on the angle offset. However, the 0.3mr we assume is sufficient for the measurement. As seen in Fig. 6, a fixed offset yields a change in slope of $\approx 1\%$ per mr, but maximum deviations from linearity of only 0.2% per mr. So a 0.3 mr offset yields a linear ε -dependence of 0.3%, which contributes to the uncertainty in G_E/G_M , but yields systematic deviations from linearity of $< 0.1\%$.

For the linearity measurement, we are again more sensitive to angle offsets that vary randomly with changing scattering angles. E04-110 [20] achieved point-to-point uncertainties in the scattering angle of 0.2 mr. The sensitivity to the proton angle varies from 0.5–1.5% per mr, yielding uncertainties in the cross section of 0.1–0.3% (largest at large ε). Table II

Source	Size	$\delta\sigma/\sigma$ total	$\delta\sigma/\sigma$ G_E/G_M	$\delta\sigma/\sigma$ linearity
Statistics [†]	0.1–0.2%	0.1–0.2%	0.1–0.2%	0.1–0.2%
Energy (fixed offset)	0.04%	0.2%	*0.1%	$\ll 0.1\%$
Energy (random)	0.04%	0.2%	0.2%	0.2%
θ_p (fixed offset)	0.30 mr	0.2–0.5%	*0.3%	$< 0.1\%$
θ_p (random)	0.20 mr	0.1–0.3%	0.1–0.3%	0.1–0.3%
Dead Time		0.1%	$< 0.1\%$	$\ll 0.1\%$
Dummy Subtraction		0.2–0.5%	*0.2%	$\ll 0.1\%$
Background Subtraction		0.1–1.0%	*0.3%	$< 0.1\%$
Radiative Corrections		1.2%	0.2%	$\sim 0.1\%$
			*0.2%	
Luminosity		0.6%	0.2%	0.2%
Proton absorption		1.0%	$\ll 0.1\%$	$\ll 0.1\%$
Acceptance		$\sim 3\%$	$\ll 0.1\%$	$\ll 0.1\%$
Efficiency		0.5%	$\ll 0.1\%$	$\ll 0.1\%$
Total		$\sim 3.7\%$	0.42–0.50%	0.38–0.47%
			*0.52%	

* Uncertainty given is on the slope rather than the individual cross sections

[†] 0.3-0.5% uncertainties for the three largest Q^2 values.

TABLE II: Projected uncertainties for the proposed measurement. The error on the extracted G_E/G_M depends on the value of G_E/G_M and is shown in Fig. 10.

summarizes the uncertainties for the extraction of the cross section, form factor ratio, and the linearity measurements.

E. Kinematics

A precise measurement of any nonlinearities will require taking data at many ε values, including several low and high ε points. This means taking data at several beam energies and using multiple linac settings in order to have sufficient measurements to be sensitive to nonlinearities at low ε . Figure 8 shows the kinematics (Q^2 vs. ε) for elastic scattering for some of the energies achievable with six proposed linac energy settings. The green lines correspond to $E_{linac}=887$ (solid), 942 (dashed), and 1002 (dotted) MeV per pass, while the light blue lines correspond to 1067 (solid), 1133 (dashed), and 1200 (dotted) MeV per pass. These are the linac energies required by E02-010, scaled up to reach a maximum energy of 6.0 GeV, rather than the 5.7 GeV in that proposal. This change is consistent with the requirements of E02-010 [32], although the measurement proposed here would not be significantly affected by running at slightly lower energies. While we have chosen to match the linac settings to those of E02-010, the experiment is compatible with other experiments that require several linac settings, with some minor changes to the specific Q^2 values where data will be taken.

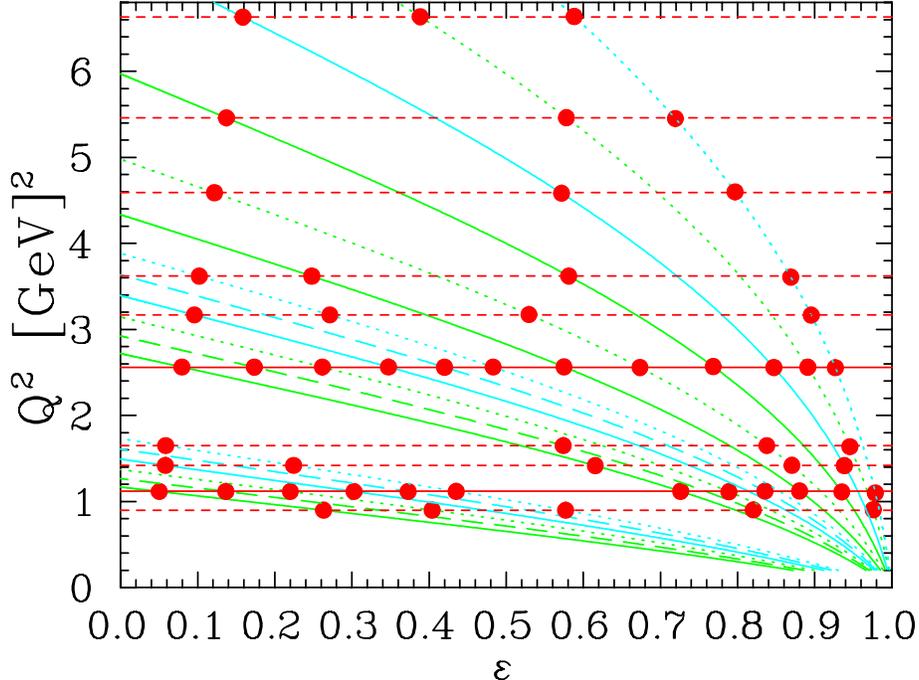


FIG. 8: The ε values that can be measured as a function of Q^2 for the available electron energies. The solid red lines indicate the Q^2 values where the nonlinearity measurements will be performed (12 ε values each), while the dashed lines indicate the additional Q^2 values where we will make precise measurements of G_E/G_M . The red circles indicate the points where measurements will be taken. The minimum ε value is determined by the minimum scattering angle of 10.5 degrees.

Using these linac energies, we can measure several points at both large and small ε -values for $Q^2=1.12$ and 2.56 GeV^2 . For the low (high) Q^2 point, we will take one-pass (two-pass) data for each of the linac settings to provide six low ε points, and then take data at six high ε values, spaced roughly uniformly up to the maximum possible value. This will provide maximum sensitivity, especially if the nonlinearities occur only at small or large ε values, as we will be able to precisely determine the slope in the linear region, and then see the effect of any nonlinearities in *multiple* data points. In addition to the linearity measurements, we will make precise extractions of G_E/G_M at $Q^2=0.90, 1.42, 1.65, 3.17, 3.62, 4.59, 5.46,$ and 6.63 GeV^2 . These data will significantly improve the existing Rosenbluth extractions of $\mu_p G_E/G_M$, and allow us to use the discrepancy between Rosenbluth and polarization to make quantitative statements on the size of the two-photon amplitudes (Sec.V C).

F. Yields

A beam of 70 μA on a 4 cm liquid hydrogen target gives a luminosity of 7.6×10^{37} which, for a 3.2 msr solid angle, means that the expected yields can be obtained by multiplying the cross sections (in fm^2/sr) by 2.4×10^9 . This yields ~ 2.4 counts/second at the lowest cross section setting for $Q^2 = 6.63$ GeV^2 , allowing a statistical uncertainty of 0.5% in five hours. The cross sections are a factor of two or more higher at all other Q^2 settings, and a factor of 10 or more higher for $Q^2 < 4$ GeV^2 , so the desired statistics, 0.1 – 0.4% , can be achieved in a few hours for each setting. See Table III for the run time and desired statistics for each

$Q^2=0.90$ (0.1% statistics)	5 × 1 hr	5 hrs	
$Q^2=1.12$	12 × 1.5 hrs	18 hrs	
$Q^2=1.42$	5 × 1.5 hrs	8 hrs	
$Q^2=1.65$	4 × 2 hrs	8 hrs	
$Q^2=2.56$ (0.2% statistics)	12 × 2.5 hrs	30 hrs	
$Q^2=3.17$	4 × 4 hrs	16 hrs	
$Q^2=3.62$	4 × 6 hrs	24 hrs	
$Q^2=4.59$ (0.3% statistics)	3 × 6 hrs	18 hrs	
$Q^2=5.46$ (0.4% statistics)	3 × 7 hrs	21 hrs	
$Q^2=6.63$ (0.5% statistics)	3 × 8 hrs	24 hrs	172 hrs
Coincidence runs	3 × 6 hrs	18 hrs	
Target boiling studies		4 hrs	
BCM calibrations		8 hrs	
Checkout/calibration		12 hrs	
Beam energy measurements	18 × 1 hr	18 hrs	60 hrs
linac changes	6 × 8 hrs	48 hrs	
pass changes	12 × 4 hrs	48 hrs	96 hrs
Total			328 hrs (14 days)

TABLE III: Beam time request. Time listed for the main data taking includes time for running on the dummy target.

setting.

V. BEAM TIME REQUEST

A. Run plan

Data will be taken with a 4 cm liquid hydrogen and an aluminum ‘dummy’ target will be used to subtract the contributions from the target endcaps. In addition to the proton inclusive data for the G_E/G_M measurement, we will take several test measurements. Runs will be taken at different beam currents in order to verify our measurement of the target heating effects, dead time, and other rate-dependent effects in the spectrometers. Data will be taken with a thin carbon target at all kinematics as a check on the target position and beam offsets. Finally, coincidence data will be taken at some settings as a check of the scattering kinematics, and as a measure of proton detection efficiency and absorption (although these corrections cancel in the ε -dependence). We can also use the coincidence data to examine the elastic proton spectrum without the backgrounds, allowing us to check the agreement between the data and the simulated elastic (and background) spectra.

Data taking for the points shown in Fig. 8 is summarized in Table III. The overhead assumed is very close to what was assumed by E02-010, which assumed 6 hours for each energy (linac change or pass change), but had 6 linac changes with only 9 additional pass changes. We request a total of 14 PAC days, including the main data taking, calibration and checkout runs, and overhead for beam energy and changes.

B. Projected Uncertainties

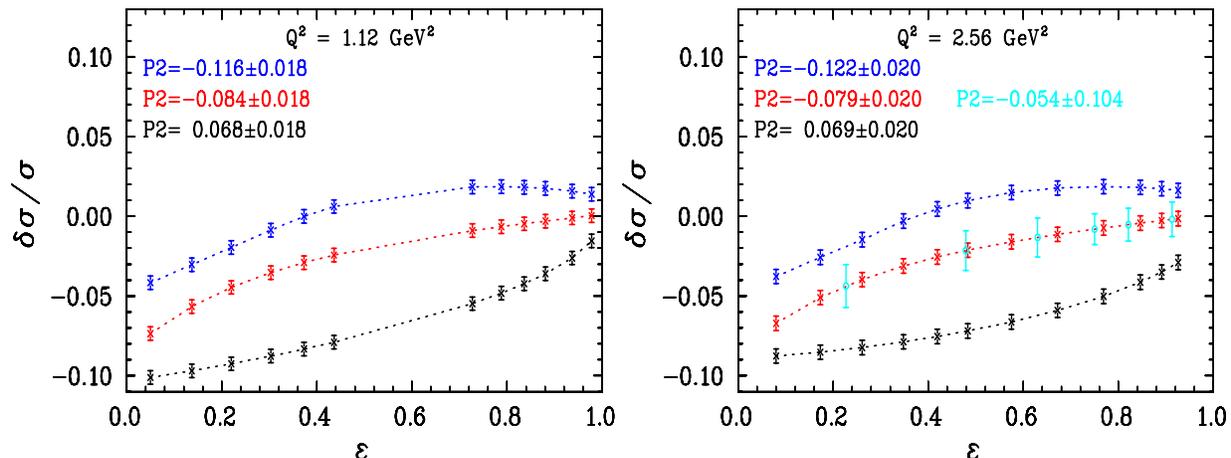


FIG. 9: The ε -dependence of the two-photon contributions to the elastic e-p cross section from calculations by Blunden, *et al.*, [12] (red), Afanasev [15] (black), and Chen, *et al.*, [14] (blue), all scaled to explain the discrepancy as described in Fig. 5. The crosses show the kinematics and projected uncertainties for the proposed $Q^2 = 1.12 \text{ GeV}^2$ measurement (left) and the $Q^2 = 2.56 \text{ GeV}^2$ (right). For each curve, the extracted P_2 and its uncertainty are also shown. The light blue points in the bottom curve show the ε values and uncertainties for the NE11 measurement at 2.5 GeV^2 (arbitrarily placed on the middle curve).

Table II summarizes the systematic uncertainties for the measurements. Separate entries are given for the total uncertainty in the absolute cross sections, the uncertainties that enter into the extraction of G_E/G_M (neglecting uncertainties that are ε -independent), and the uncertainties that enter into the linearity tests (neglecting the portions of the systematic uncertainties that vary *linearly* with ε). Figure 9 shows the kinematics for the linearity checks, along with the projected uncertainties, placed on different estimates of the two-photon corrections as described in section III. For the $Q^2 = 2.64 \text{ GeV}^2$ measurement, the uncertainty on the quadratic term (P_2 from Eq. 1) is 0.020, which yields a 4σ measurement using the estimate based on the calculation of Blunden, *et al.*, [12], a 3.5σ measurement using the estimate of Afanasev [15], and a 6σ measurement based on the calculation from Chen, *et al.*, [14]. For the $Q^2 = 1.12 \text{ GeV}^2$ measurement, $\delta P_2 = 0.018$, and P_2 is four or more standard deviations from zero for all three estimates. Note that for the real results, the statistical scatter of the data points will change the extracted value of P_2 , but not the uncertainty on P_2 .

Figure 10 shows the projected uncertainties for the proposed measurements compared to existing Rosenbluth and polarization transfer data, and the projected uncertainties for the preliminary results of E01-001. Note that the results are plotted as $(\mu_p G_E/G_M)^2$ as well as $\mu_p G_E/G_M$, since this is the more accurate way of representing the Rosenbluth uncertainties, and it is these uncertainties that limit the extraction of the two-photon amplitudes. In addition to the significant improvement in the measurement of nonlinearities, these data will also significantly improve Rosenbluth extractions of G_E/G_M . This, coupled with the reduced systematic uncertainties in the final analysis of the polarization transfer measurement [3], will allow us to extract the size of the two-photon corrections.

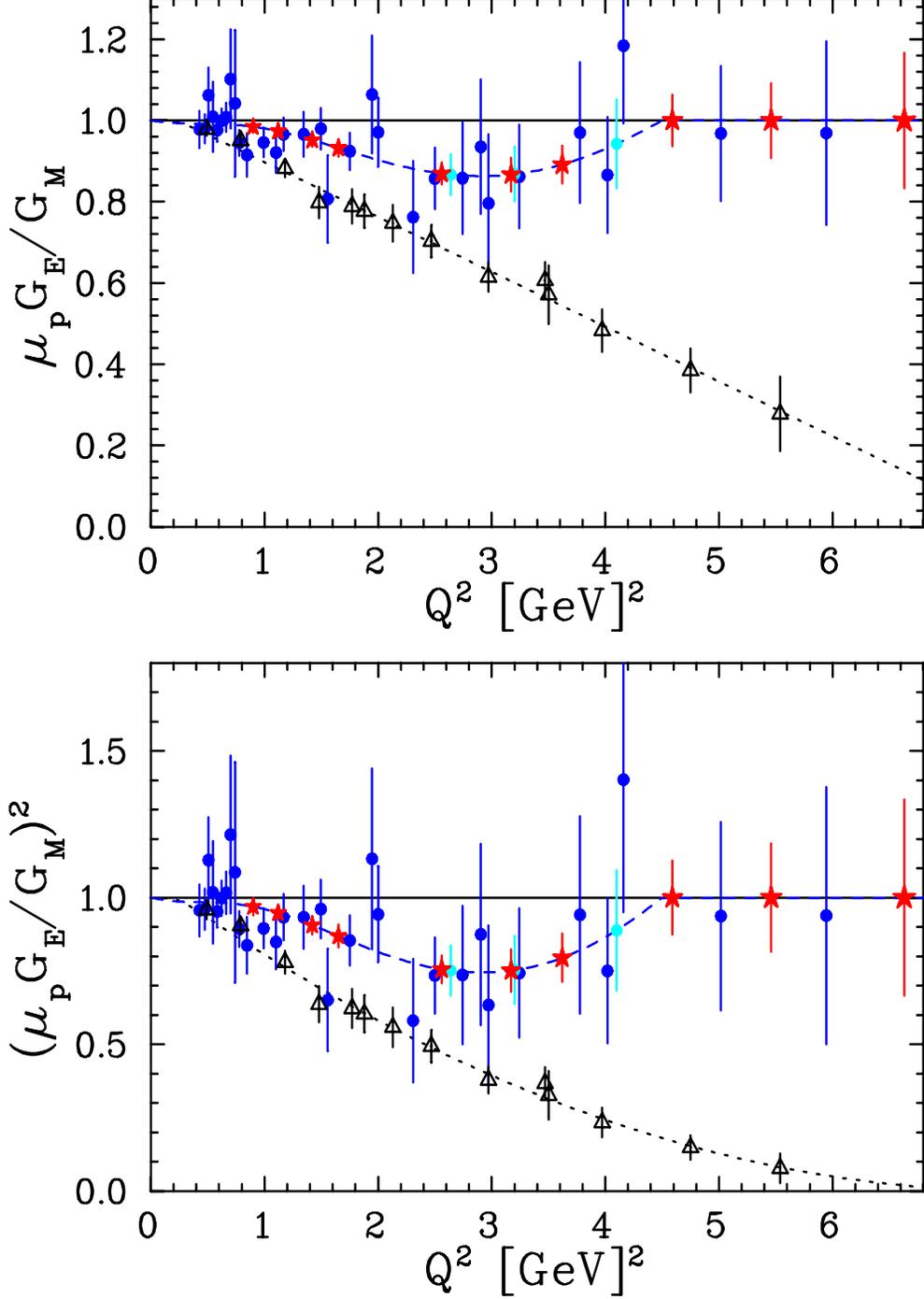


FIG. 10: Form factor ratio (top) and ratio squared (bottom) as deduced from polarization transfer (black triangles) and a global analysis of L-T separation experiments [4] (dark blue circles). The light blue circles indicate the preliminary uncertainties for E01-001, placed on the fit from the global L-T analysis. The red stars are the projected uncertainties for this proposal. Note that the low Q^2 polarization transfer data shown are from the unpublished final analysis [3], and so show the anticipated final uncertainties.

C. Extraction of two-photon amplitudes

This section summarizes the extraction of the two-photon amplitudes presented in Ref. [17], which is included with this proposal, and discusses the impact of the proposed measurements on this kind of analysis.

Using the formalism of Guichon and Vanderhaeghen [9], it is possible to express the cross section and polarization transfer results in terms of three generalized form factors, \tilde{G}_E , \tilde{G}_M , and \tilde{F}_3 , which include two-photon contributions, rather than the usual two form factors that appear in the Born approximation. Note that these form factors depend on both ε and Q^2 , and have both real and imaginary parts. In the following discussion, we will consider only the real part of these amplitudes, as the imaginary parts have negligible contributions to the cross section and polarization transfer observables. For convenience, the generalized electric and magnetic form factors are broken up into the Born form factors and a two-photon contribution:

$$\tilde{G}_E(\varepsilon, Q^2) = G_E(Q^2) + \Delta G_E(\varepsilon, Q^2), \quad (3)$$

$$\tilde{G}_M(\varepsilon, Q^2) = G_M(Q^2) + \Delta G_M(\varepsilon, Q^2), \quad (4)$$

and we define

$$Y_{2\gamma} = \mathcal{R}e\left(\frac{\nu\tilde{F}_3}{M_p^2 |G_M|}\right), \quad (5)$$

where $\nu = M_p^2 \sqrt{(1+\varepsilon)/(1-\varepsilon)} \sqrt{\tau(1+\tau)}$ (equivalent to the definition given in Ref. [9]).

The ratio that is extracted from Rosenbluth and polarization transfer experiments (assuming one-photon exchange) can be written in terms of these generalized form factors, keeping terms up to order α with respect to the Born cross section, as

$$R_{Pol} = (\tilde{G}_E/\tilde{G}_M) + (1 - \frac{2\varepsilon}{1+\varepsilon} \tilde{G}_E/\tilde{G}_M) Y_{2\gamma}, \quad (6)$$

$$R_{L-T}^2 = (\tilde{G}_E/\tilde{G}_M)^2 + 2(\tau + \tilde{G}_E/\tilde{G}_M) Y_{2\gamma}, \quad (7)$$

and the change to the reduced cross section is

$$\frac{\Delta\sigma_r}{G_M^2} \approx 2\tau \frac{\Delta G_M}{G_M} + 2\varepsilon\rho^2 \frac{\Delta G_E}{G_E} + 2\varepsilon(\tau + \rho) Y_{2\gamma}, \quad (8)$$

where $\rho = G_E/G_M$.

From Eqs. 6 and 7, we can see that it is only the $Y_{2\gamma}$ term that leads to a difference between the polarization transfer and L-T form factor ratio. Thus, this difference will allow us to determine $Y_{2\gamma}$, as was done in [9, 17]. To obtain the true form factors we must still determine ΔG_M and ΔG_E . Because the dominant term of the two-photon correction changes sign for positron-proton scattering, we can use the existing data for positron-proton scattering to constrain ΔG_E and ΔG_M , allowing an extraction of the true form factors, G_E and G_M , corrected for two-photon (and multi-photon) exchange contributions. These are form factors that can be directly connected to the structure of the proton, and which can be compared to models of the nucleon.

Such an analysis has been performed for the existing Rosenbluth and polarization transfer data [17]. The analysis is severely limited by the quality of the existing data:

(1) The analysis must assume that the entire discrepancy is related to higher-order radiative corrections such as two-photon exchange.

(2) The ε -dependence of the two-photon amplitudes is unknown. Existing analyses have assumed that the amplitudes are independent (or nearly independent) of ε .

(3) The uncertainties on the Rosenbluth extractions of $\mu_p G_E/G_M$ dominate the uncertainties (40–100%) in the extraction of the two-photon amplitudes.

While this proposal does not directly impact the first of these issues, existing positron data and recent attempts to calculate the two-photon exchange effects certainly suggest that the discrepancy is related to two-photon exchange contributions. In addition, new measurements of positron- and electron-proton scattering at low ε can be made to determine if these corrections fully explain the discrepancy.

This proposal directly addresses the other two limitations in such an analysis. Most directly, we will provide significantly better Rosenbluth measurements of $\mu_p G_E/G_M$. This will mean that instead of determining the two-photon amplitudes with uncertainties of 40–100%, we can determine them to $\lesssim 30\%$ over a wide range in Q^2 , which will yield uncertainties related to these corrections that are comparable to or smaller than the experimental uncertainties in the form factors. The uncertainty in the two-photon amplitudes is currently dominated by the large uncertainties in the Rosenbluth measurements of G_E/G_M , and this yields the largest uncertainty in the extraction of G_E/G_M . The extraction of G_M is limited by the extrapolation to $\varepsilon = 0$ coming from possible nonlinearities, which will be improved by setting better limits on the nonlinearity, and by taking data at extremely low ε values.

Table IV shows the uncertainties on G_M and G_E/G_M due to the experimental errors, the uncertainty in the two-photon amplitudes, the effect of nonlinearities on the extrapolation to $\varepsilon = 0$, and the uncertainty related to experimental uncertainties on the high ε limits from positron-electron comparisons. The uncertainty shown for the *extraction* of the two-photon amplitudes assumes that the amplitudes are ε -independent. Possible nonlinearities would also contribute to this uncertainty, which would be reduced given the improved measurements of the ε -dependence proposed here.

Form Factor	Source of uncertainty		
	Experimental	Extraction of 2γ amplitudes	Nonlinearities and e^+/e^- limits
G_M (current)	1–2%	*2–3%	2–3%
G_M (proposed)	1–2%	$\sim 1\%$	$\sim 0.5\%$
G_E/G_M (current)	4–10%	*6–13%	–
G_E/G_M (proposed)	4–10%	4–8.5%	–
* - Neglecting the uncertainty due to possible ε -dependence on the <i>extraction</i> of the amplitudes			

TABLE IV: Experimental and two-photon exchange related uncertainties in the form factors given the existing data and with the inclusion of the proposed measurements.

In addition, the improved measurements of the ε -dependence of the cross section can be used to test the assumption that two-photon amplitudes are ε -independent. This assumption is based largely on the fact that the present Rosenbluth data do not show any indication of deviations from the linear ε -dependence of the Born cross section. In Eq. 8, $\Delta G_E/G_E$

and $Y_{2\gamma}$ enter into the cross section multiplied by a factor of ε , and ΔG_M enters with no additional ε weighting. So if the amplitudes are independent of ε , then the change in the cross section will be linear in ε , and will not spoil the linearity expected from the Rosenbluth formula. However, while these two-photon contributions must yield a linear ε -dependence of approximately 5–8%, current limits allow deviations from linearity of approximately 3% (Fig. 3), more if the non-linearities occur only at large or small ε values. So while the dominant correction appears to be linear in ε , there could still be nonlinear contributions that are up to half of the size of the full effect. The present proposal would improve the limits on deviations from linearity by a factor of six, which would limit any nonlinear two-photon contribution to roughly 10% of the linear correction, making any non-linearity a small perturbation to the linear behavior assumed in this analysis.

VI. EXPERIMENTS WITH SIMILAR PHYSICS GOALS

Experiment E04-019 was approved by PAC25 to measure the ε -dependence of polarization transfer extractions of G_E/G_M . This is sensitive to the ε -dependence of the two-photon amplitude $Y_{2\gamma}$ as defined in Ref. [9]. The discrepancy can be explained with small values of $Y_{2\gamma}$, well below the sensitivity of the experiment as proposed, but E04-019 will be able to determine if there is a large ε -dependence in $Y_{2\gamma}$, or else set upper limits if no effect is observed. Because the experiment will determine the ε -dependence but not the *size* of $Y_{2\gamma}$, it will not by itself provide enough information to correct the polarization transfer results for two-photon effects. However, any information on the ε -dependence of $Y_{2\gamma}$ can be used in the global analysis described above.

There were four other proposals deferred by PAC25 that also examined two-photon exchange effects. One proposal was designed to check the polarization transfer results with a polarized target asymmetry measurement. If such a measurement were to agree with polarization transfer results, then it provides further support for the existence of the discrepancy and thus supports the case for the proposed experiment. If it were to determine that the discrepancy was caused by some problem with the polarization transfer data and that the Rosenbluth results were not significantly modified by two-photon effects, then the proposed measurements would provide the most precise data on G_E over a large range in Q^2 (Fig. 10). In addition, they would still provide much better limits on any possible non-linearities.

Three of the deferred proposals were designed to measure Born-forbidden polarization observables which provide direct access to two-photon exchange contributions. These observables are sensitive to the imaginary part of the two-photon exchange amplitudes, and so do not directly relate to the proton form factor measurements. However, they do provide entirely independent measurements of two-photon effects, and so are complementary to the measurements proposed here for testing models of the two-photon exchange effect.

VII. CONCLUSIONS

We propose to make high precision measurements of the linearity of the Rosenbluth plot at $Q^2 = 1.12$ and 2.56 GeV². Deviations from linearity would be a clear indication of deviation from the Rosenbluth formalism, and provide an additional way to constrain models of the two-photon exchange. Various calculations of the two-photon exchange corrections, small enough to be unobserved by previous measurements but large enough to explain the

discrepancy between Rosenbluth and polarization transfer, yield very different nonlinearities which can be observed as more than three to four standard deviation effects at both Q^2 values.

In addition, high precision L-T separations of G_E/G_M can be performed at several Q^2 values, allowing precise extractions of G_E/G_M from 0.9–6.6 GeV². Such high precision data can be compared to high precision polarization transfer data to determine the magnitude of the two-photon corrections as a function of Q^2 . While this data on the ε - and Q^2 -dependence of the two-photon exchange amplitudes will be very useful in constraining models of the two-photon contributions, the main goal is to extract the proton form factors. With the proposed measurements, a global analysis of Rosenbluth, polarization transfer, and positron measurements will allow us to constrain the two-photon amplitudes at the $\sim 30\%$ level; well enough to extract the form factors with uncertainties from the two-photon exchange terms that is comparable to or below the present experimental uncertainties.

We request a total of 14 days to perform the linearity checks at two Q^2 values, and high-precision Rosenbluth extractions of G_E/G_M at several Q^2 values from 0.9 to 6.6 GeV².

-
- [1] M. K. Jones et al., Phys. Rev. Lett. **84**, 1398 (2000).
 - [2] O. Gayou et al., Phys. Rev. Lett. **88**, 092301 (2002).
 - [3] V. Punjabi et al., Tech. Rep., JLab Report JLAB-PHY-03-13 (2003).
 - [4] J. Arrington, Phys. Rev. **C69**, 022201 (2004).
 - [5] B. D. Milbrath et al., Phys. Rev. Lett. **82**, 2221(E) (1999).
 - [6] D. Dutta et al. (JLab E91013), Phys. Rev. **C68**, 064603 (2003).
 - [7] J. Arrington, Phys. Rev. **C68**, 034325 (2003).
 - [8] J. Arrington, R. E. Segel, et al., Jefferson lab experiment E01-001.
 - [9] P. A. M. Guichon and M. Vanderhaeghen, Phys. Rev. Lett. **91**, 142303 (2003).
 - [10] D. Higinbotham, Tech. Rep., JLab Report JLAB-PHY-03-116 (2003).
 - [11] J. Arrington and I. Sick, in preparation.
 - [12] P. G. Blunden, W. Melnitchouk, and J. A. Tjon, Phys. Rev. Lett. **91**, 142304 (2003).
 - [13] M. P. Rekalo and E. Tomasi-Gustafsson (2003), nucl-th/0307066.
 - [14] Y. C. Chen, A. Afanasev, S. J. Brodsky, C. E. Carlson, and M. Vanderhaeghen (2004), hep-ph/0403058.
 - [15] A. Afanasev, S. Brodsky, and C. Carlson, presented at the DNP Meeting, Tuscon, AZ, Oct. 2003.
 - [16] L. W. Mo and Y.-S. Tsai, Rev. Mod. Phys. **41**, 205 (1969).
 - [17] J. Arrington, in preparation. A draft is included with this proposal.
 - [18] L. Andivahis et al., Phys. Rev. D **50**, 5491 (1994).
 - [19] R. C. Walker et al., Phys. Rev. D **49**, 5671 (1994).
 - [20] M. E. Christy et al. (2004), nucl-ex/0401030.
 - [21] C. Berger, V. Burkert, G. Knop, B. Langenbeck, and K. Rith, Phys. Lett. B **35**, 87 (1971).
 - [22] L. Camilleri et al., Phys. Rev. Lett. **23**, 149 (1969).
 - [23] J. Arrington, Phys. Rev. **C69**, 032201 (2004).
 - [24] R. R. Lewis, Phys. Rev. **102**, 537 (1956).
 - [25] S. D. Drell and M. Ruderman, Phys. Rev. **106**, 561 (1957).
 - [26] S. D. Drell and S. Fubini, Phys. Rev. **113**, 741 (1959).

- [27] N. R. Werthammer and M. A. Ruderman, Phys. Rev. **123**, 1005 (1961).
- [28] G. K. Greenhut, Phys. Rev. **184**, 1860 (1969).
- [29] W. Melnitchouk, private communication.
- [30] A. Afanasev, I. Akushevich, and N. P. Merenkov (2002), hep-ph/0208260.
- [31] M. P. Rekalov and E. Tomasi-Gustafsson (2002), nucl-th/0202025.
- [32] D. Dutta, private communication.